338

Available online at www.sciencedirect.com

SCIENCE DIRECT

ELSEVIER

Journal of Nanjing Medical University, 2008, 22(6):338–345

JNMU

www.elsevier.com/locate/jnmu

Research paper

Critical Amino Acid Residues for Nicotine 5'-Hydroxylation in Human CYP2A Enzymes☆

Xiaoyang He[a,f*], Xu Xu[b], Jian Shen[c], Li Sun[d,f], Anthony Y. H. Lu[e], Clifford Weisel[b], Junyan Hong[f]

[a]*College of Life Sciences, Shenzhen University, Shenzhen 518060,Guangdong Province,China*

[b]*Environmental Biomarker Shared Resource, The Cancer Institute of New Jersey/Environmental and Occupational Health Sciences Institute, NJ 08854, USA*

[c]*Aventis Pharmaceuticals, NJ 08807, USA*

[d]*Department of Histology & Embryology, Guilin Medical College, Guilin 541004,Guangxi Province,China*

[e]*College of Pharmacy, Rutgers University, NJ 088544, USA*

[f]*School of Public Health/EOHSI, University of Medicine and Dentistry of New Jersey, NJ 08854, USA*

Received 10 November, 2008

Abstract

Objective: We have continued previous work in which we demonstrated that #117 and #372 amino acids contributed to the high activities of human CYP2A13 in catalyzing 4-methylnitrosamino-1-(3-pyridyl)-1-butanone(NNK) and aflatoxin B1(AFB1) carcinogenic activation. The present study was designed to identify other potential amino acid residues that contribute to the different catalytic characteristics of two CYP2A enzymes, CYP2A6 and CYP2A13, in nicotine metabolism and provide insights of the substrate and related amino acid residues interactions. **Methods:** A series of reciprocally substituted mutants of CYP2A6Ile^{300} → Phe, CYP2A6Gly^{301}Ala, CYP2A6Ser^{369} → Gly, CYP2A13Phe^{300} → Ile, CYP2A13Ala^{301} → Gly and CYP2A13Gly^{369} → Ser were generated by site-directed mutagenesis/baculovirus-Sf9 insect cells expression. Comparative kinetic analysis of nicotine 5'hydroxylatin by wild type and mutant CYP2A proteins was performed. **Results:**All amino acid residue substitutions at 300, 301 and 369 caused significant kinetic property changes in nicotine metabolism. While CYP2A6Ile^{300} → Phe and CYP2A6Gly^{301}→Ala mutations had notable catalytic efficiency increases compared to that for the wild type CYP2A6, CYP2A13Phe^{300}→Ile and CYP2A13Ala^{301}→Gly replacement introduced remarkable catalytic efficiency decreases. In addition, all these catalytic efficiency alterations were caused by V_{max} variations rather than K_m changes. Substitution of #369 residue significantly affected both K_m and V_{max} values. CYP2A6Ser^{369} → Gly increase the catalytic efficiency via a significant K_m decrease versus V_{max} enhancement, while the opposite effects were seen with CYP2A13Gly^{369} → Ser. **Conclusion:**#300, #301 and #369 residues in human CYP2A6/13 play important roles in nicotine 5'-oxidation. Switching #300 or #301 residues did not affect the CYP2A protein affinities toward nicotine, although these amino acids are located in the active center. Ser^{369} to Gly substitution indirectly affected nicotine binding by creating more space and conformational flexibility for the nearby residues, such as Leu^{370} which is crucial for many hydroxylations.

Key words: CYP2A6; CYP2A13; nicotine 5'-hydroxylation; site-directed mutagenesis; crucial amino acid residue

INTRODUCTION

Nicotine is the primary compound in tobacco responsible for tobacco dependence[1]. More than 80%

☆ This work was supported by the NIH grant RO1-ES10048

*Corresponding author

E-mail address: hexy2008@szu.edu.cn

of nicotine metabolism in humans proceeds via the formation of continine[2,3]. Among the several human CYP enzymes that have been reported to be active in metabolizing nicotine, CYP2A6 has been extensively demonstrated as the principle enzyme in humans responsible for the metabolism of nicotine 5'-hydroxylation(or C-oxidation) to form cotinine, and then metabolizing cotinine to *trans*-3'-hydroxycotinine[4-8]. Many recent reports revealed that CYP2A6 polymorphisms are associated with differences in nicotine 5'-oxidation in *vitro* and in *vivo*[9-11]. It is therefore not unreasonable to propose that genetic polymorphisms in nicotine metabolism may be a major determinant of an individual's moking behaviors and thus, exposure to tobacco smoke.

On the other hand, heterologously expressed CYP2A13, one of the two functional human CYP2A subfamily members, has lower K_m values and higher V_{max}/K_m ratios than CYP2A6 when catalyzing the metabolism of nicotine and its derivate,4-(methylnitrosamino)-1-(3-pyridyl)-1-butanone(NNK)[12-15]. Several studies indicated that CYP2A13/Arg257Cys mutation resulted in an activity decrease in NNK a-hydroxylation(carcinogenic activation)[16]. Some CYP2A13 alleles were reported to be associated with lung cancer in different populations[17]. Hence, CYP2A6 and CYP2A13 may both play a very important role in metabolizing nicotine and tobacco-related carcinogens. Their activities may mediate susceptibility to lung cancer among smokers.

The present study expanded the exploration of the human CYP2A enzyme structure-activity relationship (SAR) by generating more mutants and characterizing kinetic properties of mutant and wild type CYP2A6/13 proteins in catalyzing nicotine C-hydroxylation. Three pairs of CYP2A6/13 mutant proteins were obtained with mutations at amino acid residues #300, #301 and #369, all of which lie on the substrate binding channel or relate to the heme A ring binding[18,19]. Reciprocal substitutions were generated as in our previous report[20]. Nicotine activity analysis was conducted at 10 μM and 100 μM to allow us to predict trends in changes in the kinetics of each mutant. Comparative kinetic studies among the mutants and wild type CYP2A enzymes, together with the computer modeling of the docking of nicotine into the CYP2A6 homology provided insights into the details of the structure-functional relationships of CYP2A enzymes. Crucial amino acid residues contributing to the high activity of CYP2A6/13 in the major nicotine metabolism pathway were identified.

MATERIALS AND METHODS

Chemicals, Reagents and Instruments

Ferric citrate, δ-amino-levulinic acid(δ-ALA), (-)-nicotine(>99%), (-)cotinine(~98%), cotinine-methyl-d3(99atom% D), tripotassium phosphate, NADPH and goat anti-mouse IgG conjugated with horseradish peroxidase were purchased from Sigma-Aldrich(St. Louis, MO, USA) . Methanol(>99%) and water(High purity) were from Honeywell Burdick & Jackson (Muskegon, MI, USA). $B_{AC\text{-}TO\text{-}}B_{AC}$ baculovirus/Sf9 expression system(BV system, including an expression vector $pF_{ASTBAC}1$) and cell culture media were purchased from Invitrogen(Gaithersburg, MD, USA). NADPH-P450 oxidoreductase(OR) was prepared[21] from Sf9 cell microsomes containing heterologously expressed Sprague-Dawley rat OR proteins(the cDNA was a gift from Dr. Paul E. Thomas, Rutgers University, NJ, USA). The Oasis HLB extraction cartridge was from Waters Corp. (Milford, MA, USA). Instruments used were: UV/Visible spectrophotometer(Shimadzu UV 160U, Japan), LS-5B luminescence spectrometer (PerkinElmer Co., Shelton, CN, USA), TSQ quantum triple quadrupole mass spectrometer(ThermoFinnigan, San Jose, CA).

Site-directed mutagenesis and protein expression

Site-directed mutagenesis was performed by using the wild-type CYP2A6 and CYP2A13 cDNAs as templates. Amino acid residues at positions 300, 301 and 369 were reciprocally substituted in CYP2A6 and CYP2A13 using the same approach as previously described[20]. Primers(***Table 1***) used for site-directed mutagenesis were synthesized by Integrated DNA Technologies(Coralville, IA, USA). The methods for heterologous expression, microsome preparation, protein detection and P450 contents determination were described in detail previously[20].

Table 1 **Primers used for produce desired site mutagenesis**

Primers(5'→3')	Desired mutation
CYP2A6	
2A6-300 F1:GAACCTCTTCTTTGGGGGCACCGAG	Ile^{300}→Phe
2A6-300 R2:GCCCCCAAAGAAGAGGTTC	
2A6-301 F1:ACCTCTTCATTGCGGGCACCGAGAC	Gly^{301}→Ala
2A6-301 R2:CTCGGTGCCCGCAATGAAG	
2A6-369 F1:TCCCCATGGGTTTGGCCCGCA	Ser^{369}→Gly
2A6-369 R2:GGCCAAACCCATGGGGATCACGTCT	
CYP2A13	
2A13-300 F1:TGAACCTCTTCATTGCGGGCAC	Phe^{300}→Ile
2A13-300 R2:GCCCGCAATGAAGAGGTTCAG	
2A13-301 F1:TCTTCTTTGGGGGCACTGAGAC	Ala^{301}→Gly
2A13-301 R2:CAGTGCCCCCAAAGAAGAGG	
2A13-369 F1:CCCATGAGTTTGGCCC	Gly^{369}→Ser
2A13-369 R2:GGGCCAAACTCATGGGGAGCA	

The codons to be mutated were underlined. Accession no: CYP2A6 cDNA(M33318); CYP2A13 cDNA(AF209774.1)

Nicotine 5'-hydroxylation activity assay and kinetic study

All wild type and mutant CYP2A6 and 2A13 proteins, including CYP2A6Ile^{300}→Phe, CYP2A6Gly^{301}→Ala, CYP2A6Ser^{369}→Gly, CYP2A13Phe^{300}→Ile, CYP2A13Ala^{301}→Gly and CYP2A13Gly^{369}→Ser, as well as the two wild type enzymes were used in nicotine metabolism activity analyses at two substrate concentrations(10 and 100 μmol/L). The enzyme proteins that exhibited substantial activity changes using both the lower and higher nicotine concentrations were further subjected to studies of nicotine 5'-hydroxylation kinetics. The reaction incubation system with final volume of 0.2 mL(in 50 mmol/L Tris-HCl buffer, pH 7.4) consisted of 5 pmol CYP proteins, NADPH-P450 oxidoreductase(P450: OR = 1:5 in molecular ratio), rat liver cytosol 0.5 mg/mL(as a source of cytosolic aldehyde oxidase for cotinine formation), 1 mmol/L NADPH, and nicotine with concentrations ranging from 5 to 500 μmol/L. The reaction was initiated by adding NADPH after 2-min pre-incubation at 37℃. Two hundered μL ice-cold acetone was added to terminate the reaction after 30 min. and after immediately adding 5 μL of cotinine-methyl-d_3 solution(5 μg/L in methanol) as an internal standard, the reaction solution was centrifuged at 10,000 × g for 10 min at 4℃. The supernatant was transferred into a glass tube. After adding 2 mL of 5 % tripotassium phosphate solution (w/v, pH~13), and votex mixing for 30 s., an Oasis HLB SPE cartridge(3 mL/60 mg) was used to extract the nitroaromatic/nitrosamines in the reaction solution[22]. Nitroaromatic/Nitrosamines were eluted with 1 mL of methanol/10mmol/L ammonium acetate solution(v90: 10) using a dropwise flow rate. Ten mL of the extracts or 10 ×extract dilutions of extracts of the incubation reactions that used the nicotine concentrations above 100 μmol/L were subjected to LC/MS/MS analysis.

LC/MS/MS analysis of cotinine

Chromatographic separation was performed on a Supelco Discovery HS F5 column under isocratic conditions(methanol/10 mmol/L ammonium acetate = 90:10, pH 5) using a Thermo Finnigan Surveyor System (ThermoFinnigan, San Jose, CA). The flow rate of the mobile phase was 600 μL/min; and the total run time was 7 min. A TSQ Quantum triple quadrupole mass spectrometer(ThermoFinnigan) equipped with an ion electrospray interface(ESI) was used for the mass spectrometric analysis. The ESI interface was operated in a positive ion mode with a spray voltage of 4 kV. Capillary temperature was set at 320℃. Nitrogen(99.99%, Airgas Inc., PA) was used as the sheath gas at a pressure of 49 arbitrary units and auxiliary gas at a pressure of 5 arbitrary units. Cotinine and cotinine-d_3 were measured by performing selected reaction monitoring (SRM). The most abundant ion transitions, m/z 177 > m/z 80 for cotinine and m/z 180 > m/z 80 for cotinine-d_3, was selected for identification and quantification. Argon was used as the collision gas and maintained at a constant pressure of 1.0 mTorr. The collision energy was set to 34V. Both Q1 and Q3 mass analyzers were operated under unit resolution(0.7 Da FWHM). The described conditions were optimized to achieve the best sensitivity. Xcalibur(version 1.3, ThermoFinnigan,) was used to control the LC/TSQ Quantum system, acquire, and process data. Calibration standards(0.02-800 ng/mL) were freshly prepared by the addition of different aliquots of working stock solutions(0.1 μg/mL, 10 μg/mL, and 100 μg/mL of cotinine) into water. All the calibrators were extracted in an identical manner to incubation samples as described previously. Linear regression of the peak area ratios versus concentrations was performed with 1/x weighting.

Nicotine docking

The previous generated CYP2A6 and CYP2A13 homology models[20] were used to study amino acid residues involved in the nicotine molecule binding. Substrate dockings were all carried out using the software SYBYL 6.7 and 6.8(Tripos, Inc., St. Louis, MO, USA) with MMFF94 force field(Halgren, 1996). Nicotine was energetically docked with the active site model of CYP2A6. Two binding modes, the orientations for 2'-hydroxylation and 5'-hydroxylation, were carefully studied with local energy minimization(EM)[23].

RESULTS

Expression of human CYP2A6 and CYP2A13 proteins and P450 content determination

Immunoblotting detected a single protein band with the expected molecular weight in the microsomes prepared from Sf9 cells infected by recombinant bacmid containing CYP cDNAs. No positive band was detected in the control microsomal protein prepared from the Sf9 cells infected with the vector alone(***Fig. 1A***). CO-differential spectra scanning revealed that all the wild type and mutant microsomal proteins displayed a characteristic P450 peak(***Fig. 1B***) indicating that all the recombinant cDNAs were successfully expressed. P450 contents in these samples ranged from 0.12 to 0.35 nmol/mg(data not shown).

Quantification of cotinine using LC/MS/MS

Cotinine and cotinine-d_3 were eluted at~2.7 min. The LC/MS/MS provided excellent linearity over 4-5 orders of magnitude for cotinine. The regression r^2 value of the calibration curve was greater than 0.998 in cotinine concentration range of 0.02-800 ng/mL(***Fig. 2***).

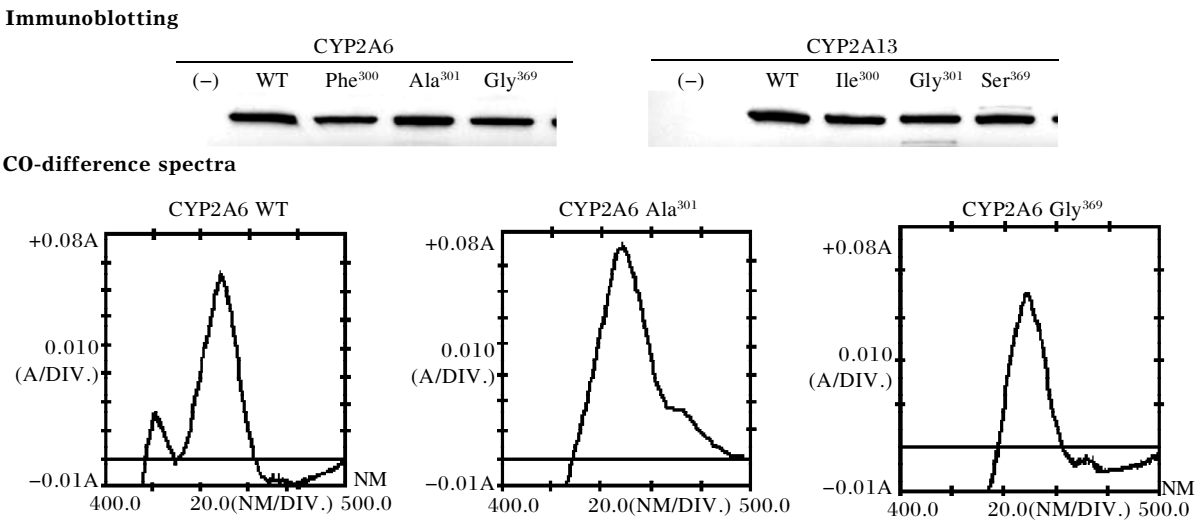

Sf9 cells were infected with recombinant bacmids containing CYP2A6WT, CYP2A6Phe^{300}, CYP2A6Ala^{301} and CYP2A6Gly^{369} as well as CYP2A13WT, CYP2A13Ile^{300}, CYP2A13Gly^{301} and CYP2A13Ser^{369} cDNAs for 72 h, respectively. The bacmid vector without cDNA was transferred into Sf9 cells as(–) control. Each 0.5 mg microsomal protein of above cells was loaded for immunoblotting. A. From left to right: control, CYP2A6-WT, Phe^{300}, Ala^{301} Gly^{369} mutants; control, CYP2A13-WT, Ile^{300}, Gly^{301} and Ser^{369} mutants. The microsomal proteins were adjusted to 2 mg/mL for CO-differential studies. B.Characteristic 450 nm absorptions of CYP2A6s(from left to right): CYP2A6WT, CYP2A6Ala^{301} and CYP2A6Gly^{369}. Each microsomal protein represented the P450 peak indicating that all construct cDNAs were expressed successfully.

Fig. 1 Heterologously expression of recombinant CYP2A6 and 2A13 cDNAs in Sf9 cells

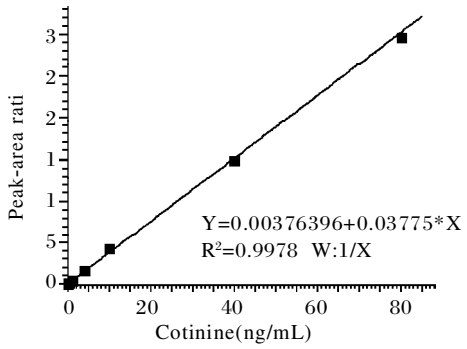

The LC/MS/MS analysis provided an excellent linearity with nearly five orders of magnitude for cotinine detection. From 0.02 to 800 ng/mL of cotinine concentrations, value of the regression coefficient r^2 for the calibration curve was greater than 0.99.

Fig. 2 Calibration curve for cotinine HPLC-MS detection

Nicotine 5'-hydroxylation and kinetic analysis

Three independent experiments from two sets of expressed samples subjecting nicotine 5'-hydroxylation activity analysis under 10 and 100 μmol/L nicotine concentrations confirmed substantial activity changes caused by the reciprocal amino acid residue substitutions. While the substitutions in CYP2A6 caused an increase in the catalytic activity, all the substitutions in CYP2A13 caused the opposite effect(***Fig. 3***). Thus, further kinetic analyses were performed with all the six mutants. For CYP2A6 proteins, three-separate experiments were conducted due to its important role in the clearance of nicotine from the human body. For the other CYP2A13 enzymes, two separate tests were carried out. The K_m difference between wild-type CYP2A6 and CYP2A13 was about 2.4 fold(62.52 μmol/L for CYP2A6 versus 26.01 μ mol/L for CYP2A13, respectively) and the V_{max} difference between these two enzymes was approximately 4 fold[6.53 nmol/(min • nmol) of CYP2A6 versus 24.51 nmol/(min • nmol) of CYP2A13]. The K_m and V_{max} differences resulted in about a 10-fold catalytic efficiency difference between these two human CYP2A members in catalyzing nicotine 5'-hydroxylation(***Table 2***). It has been demonstrated in vitro that heterologously expressed human CYP2A13 is a more efficient catalyst than CYP2A6 for nicotine metabolism. The key amino acid residues that contribute to the significant catalytic efficiency difference were identified by comparing the kinetic properties of mutants to their corresponding wild-type CYP enzymes. Data in ***Table 2*** showed that substitution of #300 or #301 residues in both CYP2A members caused notable catalytic efficiency changes, mainly by altering V_{max} rather than affecting K_m. Catalytic efficiency(K_{cat}) of CYP2A6Phe^{300} and CYP2A6Ala^{301} variants were increased about 2 folds because of the significant increases in their V_{max} values[12.73 ± 0.40, 15.53 ± 0.68 versus 6.53 ± 0.65 nmol/(min • nmol) for CYP2A6 WT, $P < 0.05$], while the K_{cat} values of CYP2A13Ile^{300} and CYP2A13Gly^{301} mutants decreased because of a near 3-fold V_{max} decrease compared to that for CYP2A13[6.48 and 9.38 versus 24.51 nmol/(min• nmol) for CYP2A13 WT]. Thus, residues 300 and 301 play an important role in nicotine 5-hydroxylation by

the two CYP2A members.

Of particular note is the fact that substitution of the residue #369, which is not located in the enzyme active site and is not directly involved in substrate binding in either CYP2A6 or CYP2A13, caused significant changes in both K_m and V_{max} values(***Table 2***). CYP2A6Gly^{369} mutant increased the catalytic efficiency with the combination of a significant K_m decrease and a significant V_{max} increase[39.94 ± 2.36 μmol/L and 12.88 ± 0.54 nmol/(min • nmol) versus 62.52 ± 5.77 μmol/L and 6.53 ± 0.65 nmol/(min • nmol) for the CYP2A6 WT, $P < 0.05$ in two-tails *t*-test]. In contrast, the CYP2A13 Ser^{369} mutant exhibited a remarkable catalytic effi-ciency decrease by increasing K_m and decreasing V_{max} values simultaneously[26.01 μmol/L and 24.51 nmol/(min • nmol) versus 92.50 μmol/L and 11.66 nmol/(min • nmol) for the CYP2A13 WT]. Experimental data indicated that residue #369 is a critical amino acid in the control of nicotine 5'-hydroxylation by human CYP2A6 and CYP2A13.

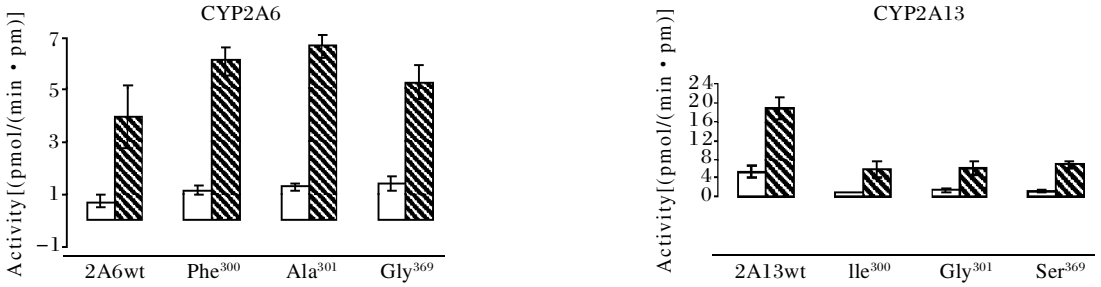

10 or 100 μmmol/L nicotine was incubated with 5 pmol CYP protein, OR(P450:OR=1:5 in molecular ratio) and cytosol. The reaction was initiated by adding NADPH. Incubation was carried out at 37℃ for 30 min. The metabolite cotinine formation activities at lower(10mmol/L) and higher(100 μmol/L) nicotine concentrations presented constant increase for all CYP2A6 mutants and decrease for all CYP2A13 mutants. Data present the mean ± SD of three separated experiments from two batches of expressed protein samples.

Fig. 3 Nicotine 5'-hydroxylation activity of CYP2A6 and CYP2A13 proteins

Table 2 **Kinetic parameters of heterologously expressed human CYP2A6s and CYP2A13s in nicotine 5'-oxidation**

Enzymes	Km (μmol/L)	Vmax[nmol/(min • nmol)]	Kcat(Vmax/Km)
CYP2A6			
WT	62.52 ± 5.77	6.53 ± 0.65	0.10
Ile300Phe	72.47 ± 2.57	12.73 ± 0.40*	0.18
Gly301Ala	68.91 ± 10.63	15.53 ± 0.68*	0.23
Ser369Gly	39.94 ± 2.36*	12.88 ± 0.54*	0.32
CYP2A13			
WT	26.01	24.51	0.94
Phe300Ile	48.18	6.48	0.13
Ala301Gly	35.15	9.38	0.27
Gly369Ser	92.50	11.66	0.13

*$P < 0.05$. Data are presented as mean ± SD of 3 to 4 separated experiment results for CYP2A6s and means of 2 independent analyses for CYP2A13s .

Nicotine docking analysis

Enzyme homology modeling based on released X-ray data is an economical and convenient tool, giving us basic insights into the substrate and related active site residues. In addition, recently released CYP2A6 and CYP2A13, as well as some of their substrates bond proteins, crystal structures have provided valuable data about residue-residue or substrate-residue interactions. It is infeasible to crystallize each substrate bond in CYP2A proteins or each CYP2A mutant protein in the investigation of enzyme structure-function relationships. Energetically docked nicotine with the active site model of CYP2A6 revealed two orientating modes of nicotine for 2'-hydroxylation(***Fig. 4A***) and 5'-hydroxylation (***Fig. 4B***). The figures present the view of the heme plane in the bottom of the substrate binding pocket. The nicotine molecule is incorporated in the binding pocket with its imidazole ring down to the heme active center. The closest distance from of heme center iron to the nicotine 2'-C is around 1Å longer than that to the 5'-C. The 5'binding mode is also energetically more favorable than the 2'-binding mode, which is consistent with the differential activities between the 5'-and 2'-hydroxylations in nicotine metabolism.

Residue #300 is located above the substrate binding pocket and in much closer contact with the upwardardly

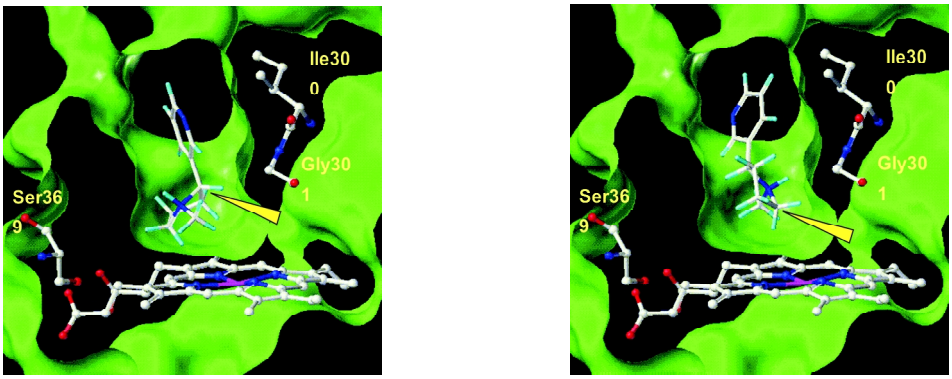

A B

As the yellow arrows point out, there are two binding modes for nicotine(A)2'-hydroxylation and (B)5'-hydroxylation. The 5'-binding mode is energetically more favorable than the 2' binding mode, which is consistent with the differential activities between the 5'- and 2'-hydroxylations in nicotine metabolism. Residue #369 is not a part of the binding pocket, but #300 and #301 are. However, the Ser^{369} to Gly substitution creates more space and conformational flexibility for the nearby residues, such as Leu^{370}, which is crucial for many hydroxylations. The upper position Ile^{300} → he can provide an additional p-stacking toward the nicotine aromatic ring.

Fig. 4 Energetically docked nicotine with the active site model of CYP2A6

facing nicotine aromatic ring. The Phe residue in this position is part of the multiple-Phe cluster "roof" in wild type CYP2A13[19] and appears be more favored by the nicotine binding in CYP2A6. The CYP2A6Ile^{300} → Phe substitution produced an extra nicotine-Phe^{300} π-stacking that may result in a catalytic activity increase toward nicotine 5'-hydroxylation. Substitution of CYP2A6Gly^{301} → Ala narrowed the bottom space of the substrate binding center and the larger Ala residue side chain may better fit the nicotine 5'-hydroxylation orientation mode that induced a catalytic efficiency increase.

Residue #369 is not a part of the substrate binding pocket. However, the Ser^{369}→Gly substitution creates more space for H_2O molecules to enter and brings more conformational flexibility for the nearby residues, such as Leu370, which is highly conserved and is crucial for many hydroxylations[24]. Together with the kinetic data, amino acid residues #369 is critical for the CYP2A6 and CYP2A13 kinetic property difference in nicotine 5'-hydroxylation.

DISCUSSION

Kinetic parameters have been determined previously for cotinine formation by P450 CYP2A6 and CYP2A13. Many reported K_m values from liver microsomes or heterologously expressed protein studies ranged from 11 to 144 μM for CYP2A6[6,7,15,25] and 22 to 74 μM for CYP2A13[13,15]. One explanation for the different K_m values reported for P450 CYP2A6/13 is that in the previous studies, different ways were used to monitor the nicotine 5'-oxidation. Cotintine formation, for instance, is commonly used to measure nicotine 5-oxidation, while the iminium ion formation rates are quite often monitored nowadays, as cotinine formation is not a measure of total nicotine 5-oxidation[15]. The apparent kinetic constant for nicotine 5-hydroxylation by CYP2A13 obtained in the present study is reasonably consistent with our previous report (26.0 μmol/L versus 20.0 μmol/L[13], although different cotinine analysis methods were applied. For CYP2A6, we obtained a K_m value of 62.52 ± 5.77 μmol/L in the parallel studies. That the K_m for CYP2A13 is about half the value for CYP2A6, as well as the V_{max} of CYP2A13 is 4-fold higher than that for CYP2A6 is in very good agreement with the report of Murphy and co-workers[15]. In conclusion, experimental data characterized CYP2A13 as a more efficient catalyst of nicotine 5'-oxidation than is CYP2A6.

The recent enzyme protein X-ray structure analysis revealed that both CYP2A6 and 2A13 have a planer, highly hydrophobic, phenylalanine rich active site[18,19,26]. CYP2A6, which has a 15-20% smaller active site volume than that of CYP2A13[18], possessing a ~10-fold higher activity toward coumarine 7-hydroxylation[12], suggests that a smaller substrate binding site volume in the CYP2A enzyme appears more complimentary to the compact, small planer substrate. In another respect, larger active site CYP2A13 is more likely to favor molecules like nicotine, NNK, NNN, AFB1 and phenacetin[12,13,26,27]. Obviously, some residues in the 32 different amino acid gaps in CYP2A6/13 account for the differences in substrate specificity and metabolism. #300 and #301 residues play an important role in adapting to the fitting of coumarin, indole or indole derivatives, and phenacetin[26,28,29]. Substitutions of these two residues in either CYP2A6 or CYP2A13 altered enzyme activities toward nicotine 5'-hydroxylation. Similar to our previous observation in coumarin 7-

hydroxylation by CYP2A6/13 [data not shown], the larger Ala^{301} side chain possessed a better fit for nicotine 5'-hydroxylation. Compared to the wild type proteins, the CYP2A6Ala^{301} mutant increased, while CYP2A13Gly^{301} decreased the nicotine to continine conversion. However, the effect of the Phe^{300} substitution on nicotine 5'-hydroxylation could not be explained by the changes in active site volume of the CYP2As. Ile300 → Phe actually enlarged the active site volume in CYP2A6. But this mutation resulted a catalytic efficiency increase in nicotine 5'-hydroxylation. In CYP2A13, Phe^{300} → Ile perturbed the six Phe(#107, #111,#118 #209, #300 and #481) cluster "roof"[19] and caused a cotinine formation decrease. Substrate docking analysis indicated that the nicotine aromatic ring on the distal side of the heme plane is π-stack with Phe^{300}. The opposite trends between CYP2A6 Phe^{300} (increase) and CYP2A13Ile^{300}(decrease) catalytic efficiency changes in nicotine 5-hydroxylation revealed that the residue #300 related π-π stacking, electron transitions and some edge-to face interactions with aromatic ligands play a priority role, rather than the side chain stereo effect. In addition, the effects of all #300 and #301 mutations on nicotine 5'-hydroxylation are primarily reflected in changes in V_{max} rather than K_m, suggesting orientation of the ligand may be related to catalysis rather than ligand affinity.

Extensive structure-activity relationship studies demonstrated that key amino acid residues are generally substrate-dependent. For example, switching #208 residues in CYP2A6 and CYP2A13 does affect enzyme catalytic properties in phenacetin metabolism, but not in coumarin 7-hydroxylation[20, 25]. Residue #369 in CYP2As plays an important role in substrate dependence similar to the residue #208. Substitution of #369 residues between CYP2A6 and CYP2A13 caused significant K_{cat} changes in nicotine 5'-hydroxylation but not in coumarin 7'-hydroxylation. Residue #369 is far from the active site and its side chain is hence somewhat distant from the nicotine molecule. In CYP2A6, Ser^{369} is found orientated toward the proximal side of the heme and interacts with the propionate A-ring[18]. Substitution of Ser^{369} to Gly instead the serine side chain hydroxyl group - propionate H-bond to a water molecule mediated interaction. The H_2O is stabilized by both the backbone amine and carbonyl of residue Leu^{370}. The most recent X-ray studies on CYP2A6 208/300/301/369 quadruple mutant crystal structure indicate that CYP2A6 Ser^{369} Gly substitution leads the Leu^{370} side chain to more favor the CYP2A13-like position/orientation and contributes to the phenacetin O-deethylation increase[26]. The concurring nicotine 5'-hydroxylation increased by CYP2A6Gly^{300} compared to CYP2A6 and decreased by CYP2A13Ser^{300} compared to CYP2A13 observed in the present study demonstrates that Gly at position 369 is more favored in nicotine metabolism by CYP2A enzymes.

Experimental assays of the nicotine 5'hydroxylation kinetics together with the computer modeling explored insights into CYP2A enzyme structure and stereoselectivity, as well as nicotine metabolism activity relationships. The ability of CYP2A enzymes to metabolize substrates is largely the culmination of steric effects of the substituted side chains themselves and their effects on the positions of adjacent side chains. Further investigations will determine whether these same residues are responsible for differences in selectivity for other CYP2A ligands, like the procarcinogens NNK, AFB1.

References

[1] Henningfield JE, Miyasato K, Jasinski DR. Abuse liability and pharmacodynamic characteristics of intravenous and inhaled nicotine. *J Pharmacol Exp Ther* 1985; 234:1-12.

[2] Benowitz NL, Jacob P 3rd. Metabolism of nicotine to cotinine studied by a dual stable isotope method. *Clin Pharmacol Ther* 1994; 56:483-93.

[3] Benowitz NL, Jacob P 3rd, Fong I, Gupta S. Nicotine metabolic profile in man: comparison of cigarette smoking and transdermal nicotine. *J Pharmacol Exp Ther* 1994; 268:296-303.

[4] Flammang AM, Gelboin HV, Aoyama T, Gonzalez FJ, McCoy GD. Nicotine metabolism by cDNA-expressed human cytochrome P-450s. *Biochem Arch* 1992; 8: 1-8.

[5] Hukkanen J, Jacob P 3rd, Benowitz NL. Metabolism and disposition kinetics of nicotine. *Pharmacol Rev* 2005; 57:79-115.

[6] Messina ES, Tyndale RF, Sellers EM. A major role for CYP2A6 in nicotine C-oxidation by human liver microsomes, *J Pharmacol Exp Ther* 1997; 282:1608-14.

[7] Nakajima M, Yamamoto T, Nunoya K, Yokoi T, Nagashima K, Inoue K, *et al.* Role of human cytochrome P4502A6 in C-oxidation of nicotine. *Drug Metab Dispos* 1996; 24:1212-7.

[8] Nakajima M, Yamamoto T, Nunoya K, Yokoi T, Nagashima K, Inoue K *et al.* Characterization of CYP2A6 involved in 3′-hydroxylation of cotinine in human liver microsomes. *J Pharmacol Exp Ther* 1996; 277:1010-5.

[9] Inoue K, Yamazaki H, Shimada T. CYP2A6 genetic polymorphisms and liver microsomal coumarin and nicotine oxidation activities in Japanese and Caucasians. *Arch Toxicol* 2000; 73:532-9.

[10] Nakajima M, Fukami T, Yamanaka H, Higashi E, Sakai H, Yoshida R, *et al.* Comprehensive evaluation of variability in nicotine metabolism and CYP2A6 polymorphic alleles in four ethnic populations. *Clin Pharmacol Ther* 2006; 80:282-97.

[11] Xu C, Rao YS, Xu B, Hoffmann E, Jones J, Sellers EM, *et al.* An in *vivo* pilot study characterizing the new CYP2A6*7, *8, and *10 alleles. *Biochem Biophys Res Commun* 2002; 290: 318-24.

[12] Su T, Bao Z, Zhang QY, Smith TJ, Hong JY, Ding X. Human cytochrome P450 CYP2A13: Predominant expression in the respiratory tract and its high efficiency metabolic activation of a tobacco-specific carcinogen, 4-(methylnirosamino)-1-(3-pyridyl)-1-butanone. *Cancer Res* 2000; 60: 5074-9.

[13] Jalas JR, Ding X, Murphy SE. Comparative metabolism of the tobacco-specific nitrosamines 4-(methylnitrosamino)-1-(3-pyridyl)-1-butanone and 4-(methylnitrosamino)-1-(3-pyridyl)-1-butanol by rat cytochrome P450 2A3 and human cytochrome P450 2A13. *Drug Metab Dispos* 2003; 31:1199-202.

[14] Bao Z, He XY, Ding X, Prabhu S, Hong JY. Metabolism of nicotine and cotinine by human cytochrome P450 2A13. *Drug Metab Dispos* 2005; 33: 258-61.

[15] Murphy SE, Raulinaitis V, Brown KM. Nicotine 5′-hydroxylation and methyl oxidation by P450 enzymes. *Drug Metab Dispos* 2005; 33:1166-73.

[16] Zhang X, Chen Y, Liu Y, Ren X, Zhang QY, Gaggana M, *et al.* Single nucleotide polymorphisms of the human cyp2a13 gene: evidence for a null allele. *Drug Metab Dispos* 2003; 31:1081-5.

[17] Wang H, Tan W, Hao B, Miao X, Zhou G, He F, *et al.* Substantial reduction in risk of lung adenocarcinoma associated with genetic polymorphism in CYP2A13, the most active cytochrome P450 for the metabolic activation of tobacco-specific carcinogen NNK. *Cancer Res* 2003; 63:8057-61.

[18] Yano JK, Hsu MH, Griffin KJ, Stout CD, Johnson EF. Structures of human microsomal cytochrome P450 2A6 complexed with coumarin and metahoxalen. *Nat Struct Mol Biol* 2005; 12: 822-3.

[19] Smith BD, Sanders JL, Porubsky PR, Lushington GH, Stout CD, Scott EE. Structure of the Human Lung Cytochrome P450 2A13. *J Biol Chem* 2007; 282:17306-13.

[20] He XY, Shen J, Hu WY, Ding X, Lu AY, Hong JY. Identification of Val117 and Arg372 as critical amino acid residues for the activity difference between human CYP2A6 and CYP2A13 in coumarin 7-hydroxylation. *Arch Biochem Biophys* 2004; 427:143-53.

[21] Williams DE, Becker RR, Potter DW, Guengerich FP, Buhler DR. Purification and comparative properties of NADPH-cytochrome P-450 reductase from rat and rainbow trout: differences in temperature optima between reconstituted and microsomal trout enzymes. *Arch Biochem Biophys* 1983; 225: 55-65.

[22] Xu X, Iba MM, Weisel CP. Simultaneous and sensitive measurement of anabasine, nicotine, and nicotine metabolites in human urine by liquid chromatography-tandem mass spectrometry. *Clin Chem* 2004; 50:2323-30.

[23] Shen J, Borcherding D. The computational differentiation of binding modes for CDK2 bound purine analogs. *Med Chem Res* 2003; 12: 435-43.

[24] Jalas JR, Seetharaman W, Hecht SS, Murphy SE. Molecular modeling of CYP2A enzymes: application to metabolism of the tobacco-specific nitrosamine 4-(methylnitrosamino)-1-(3-pyridyl)-1-butanone (NNK). *Xenobiotica* 2004; 34:515-33.

[25] Yamazaki H, Inoue K, Hashimoto M, Shimada T. Roles of CYP2A6 and CYP2B6 in nicotine C-oxidation by human liver microsomes. *Arch Toxicol* 1999; 73: 65-70.

[26] Devore NM, Smith BD, Urban MJ, Scott EE. Key resudues controllling phenacetin metabolism by human cytochrone P450 2A enzymes. *Drug Meatb Dispos* 2008 Sep 8. [Epub ahead of print].

[27] He XY, Tang L, Wang SL, Cai QS, Wang JS, Hong JY. Efficient activation of aflatoxin B1 by Cytochrome P450 2A13, an enzyme predominantly expressed in human respiratory tract. *Intl J Cancer* 2006; 118: 2665-71.

[28] Kim D, Wu ZL, Guengerich FP. Analysis of coumarin 7-hydroxylation activity of cytochrome P450 2A6 using random mutagenesis. *J Biol Chem* 2005; 280: 40319-27.

[29] Sansen S, Hsu MH, Stout CD, Johnson EF. Structural insight into the altered substrate specificity of human cytochrome P450 2A6 mutants. *Arch Biochem Biophys* 2007; 464:197-206.